Finite Boundary Layer, Mach Number 1 to 10," AFFDL RTD-TDR-63-4268, Dec. 1964, Air Force Flight Dynamics Lab.

[6] Miles, J. W., "On Panel Flutter in the Presence of a Boundary Layer," *Journal of the Aerospace Science*, Vol. 26, 1959, pp. 81–93.

[7] McClure, J. D., "On Perturbed Boundary Layer Flows," Fluid Dynamics Research Lab. Rept. 62-2, MIT, Cambridge, Mass., June 1962.

[8] Anderson, W. J. and Fung, Y. C., "The Effect of an Idealized Boundary Layer on the Flutter of Cylindrical Shells in Supersonic Flow," SM 62-49, California Institute of Technology, Pasadena, Calif., 1962.

[9] Olson, M. D., "On Comparing Theory and Experiment for the Supersonic Flutter of Circular Cylindrical Shells," AFOSR 66-0944, Graduate Aeronatucal Lab., California Institute of Technology, Pasadena, Calif., June 1966.

[10] Zeydel, E. F. E., "Study of the Pressure Distribution on Oscillating Panels in Low Supersonic Flow with Turbulent Boundary Layer," NASA CR-691, Feb. 1967, Georgia Institute of Technology.

[11] Dowell, E. H. and Voss, H. M., "Experimental and Theoretical Panel Flutter Studies in the Mach Number Range of 1.0 to 5.0," AFFDL ASD-TDR-449, The Boeing Co., 1963.

[12] Benjamin, T. B., "Shearing Flow Over a Wavy Boundary," *Journal of Fluid Mechanics*, Vol. 6, Pt. 2, pp. 161–205, 1959.

[13] Landahl, M. T., "On the Stability of a Laminar Incompressible Boundary Layer Over a Flexible Surface," *Journal of Fluid Mechanics*, Vol. 13, 1962, Pt. 14, pp. 609–632.

[14] Graham, E. W. and Graham, B. B., "Effect of a Shear Layer on Plane Waves of Sound in a Fluid," *Journal of the Acoustical Society of America*, Vol. 46, No. 1, Jan. 1969, pp. 169–175.

[15] Miles, J. W., "On the Generation of Surface Waves by Shear Flows. Part 5," *Journal of Fluid Mechanics*, Vol. 30, Pt. I, pp. 163–175, 1967.

[16] Dowell, E. H., "Generalized Aerodynamic Forces on a Flexible Plate Undergoing Transient Motion in a Shear Flow with an Application to Panel Flutter," AIAA Paper 70-76, New York, Jan. 1970.

[17] Liepmann, H. W. and Roshko, A., *Elements of Gas Dynamics*, Wiley, New York, 1957.

[18] Dowell, E. H., "Generalized Aerodynamic Forces on a Flexible Plate Undergoing Transient Motion," *Quarterly of Applied Mathematics*, Vol. 24, No. 4, Jan. 1967, pp. 331–338.

[19] Dowell, E. H., "Nonlinear Oscillations of a Fluttering Plate II," *AIAA Journal*, Vol. 5, No. 10, Oct. 1967, pp. 1856–1862.

[20] Ventres, C. S. and Dowell, E. H., "Comparison of Theory and Experiment for Nonlinear Flutter of Loaded Plates," *AIAA Journal*, Vol. 8, No. 11, Nov. 1970, pp. 2022–2030.

[21] Dowell, E. H., "Theoretical-Experimental Correlation of Plate Flutter Boundaries at Low Supersonic Speeds," *AIAA Journal*, Vol. 6, No. 9, Sept. 1968, pp. 1810–1811.

MAY 1971 AIAA JOURNAL VOL. 9, NO. 5

Jet Aircraft Air Pollutant Production and Dispersion

JOHN B. HEYWOOD,* JAMES A. FAY,† AND LAWRENCE H. LINDEN‡
Massachusetts Institute of Technology, Cambridge, Mass.

In this paper two aspects of pollution from jet engines are considered in detail. Firstly, it is shown that at or near full load, the most important air pollutants are nitric oxide and soot, and the production processes of these two pollutants are then discussed. A kinetic analysis shows that nitric oxide is formed mainly in the combustor primary zone, in regions of the flow where the equivalence ratio is greater than about 0.8, and that freezing occurs as the gas is diluted and cooled in the secondary zone. Calculated results for nitric oxide concentrations in the combustion products are presented and compared with existing experimental data. The mechanisms important in the formation of carbon in the fuel-rich regions of the primary zone are reviewed. The oxidation of this carbon in the remainder of the combustor is then considered, and the oxidation rates attainable within the combustor are computed from existing rate data. Secondly, the dispersion of the exhaust plume in the atmosphere is analyzed, the two effects considered being the entrainment of surrounding air due to turbulent motion of the jet and the motion induced by the buoyancy of the trail. For short times, mixing proceeds as in ordinary wakes; for longer times, mixing is dominated by motion induced by buoyancy.

Introduction

THE production of pollutants in aircraft jet engines and their dissemination in the atmosphere are certainly matters of public concern. A recent survey[1] concludes that "in the vicinities of air terminals, however, the density of pollutant emission by aircraft and the resulting pollutant concentrations are comparable to emission densities and concentrations in adjacent communities of the same pollutants from other sources. Thus, the principal impact of aircraft emissions is local in nature and is expected to become more severe in future years. It is also likely that aircraft emissions will constitute a more significant portion of community-wide pollutant loadings as new aircraft are introduced and as emissions from other sources are reduced." If the emissions from aircraft are averaged over a metropolitan area, their present contribution is insignificant compared with all other sources combined.[2–4] However, aircraft emissions, especially during approach, taxi, and takeoff operations, are confined to a small segment of a metropolitan area and in this respect should be considered a localized source, like a power plant, rather than widely distributed sources, such as automobiles or home heating units. Reference 1 notes that "there are a number of major air terminals at which residential areas are located along an extension of a runway or within a mile or less of the end of the runway. . . . Residents of such an area may ex-

Presented as Paper 70-115 at the AIAA 8th Aerospace Sciences Meeting, New York, January 19–21, 1970; submitted March 16, 1970; revision received December 7, 1970. This research was supported by NASA Grant NGR 22-009-378. The data presented in Fig. 8 were obtained by one of our students, T. Gilmore, and his contribution is gratefully acknowledged.

* Associate Professor of Mechanical Engineering. Member AIAA.

† Professor of Mechanical Engineering. Associate Fellow AIAA.

‡ NSF Fellow. Student Member AIAA.

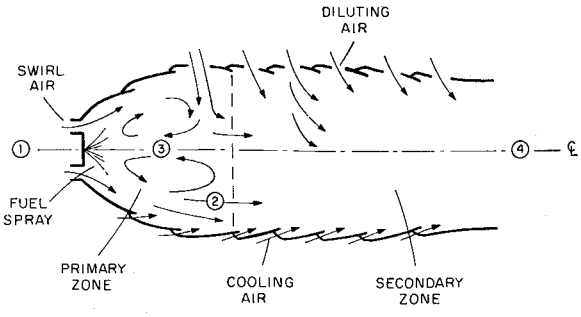

Fig. 1 Cross section of typical combustor liner: upper half shows flow through diluting air holes; lower half shows film-cooling air.

perience concentrations significantly higher than those predicted by the area source model."

The information which is needed to assess the hazards of aircraft pollution and examine possible methods for its control can be conveniently divided into the following categories: 1) the nature and amount of possibly harmful constituents of the exhaust of an aircraft gas turbine engine under various operating conditions; 2) the fundamental physical processes controlling the production of pollutants in the gas turbine combustor; 3) the relationship between the ambient level of these pollutants at various distances and directions from an airport and the aircraft traffic density, traffic pattern, and local meteorological conditions; and 4) the effect of pollutants at these ambient levels on human, animal, and plant life and also property damage. This paper is concerned with certain aspects of items 2 and 3.

The principal pollutants emitted from jet engines are NO, CO, hydrocarbons, and particulates.[4-6] When expressed as a mass percentage of fuel burned, each of these pollutants is emitted in amounts usually between 0.1% and 1.0% under most conditions of operation.[1] Emissions of CO and hydrocarbons are especially high during idle and taxi operations, while NO and particulate emissions are usually greatest during takeoff and landing.

It is commonly believed that the formation of particulates occurs in the rich primary combustion zone of the combustor[7] while NO is formed in near-equilibrium proportions in the combustion chamber but does not reconvert to N_2 and O_2 in the subsequent expansion through the turbine.[8] (We will consider these two pollutants later in this paper.) The excessive CO and hydrocarbons during idle are not a result of a rich over-all mixture, as is encountered in the automotive engine, but occur with low over-all equivalence ratios of about 0.1.

The contribution of aircraft pollutants to ambient levels in urban areas has been compared to other sources on the basis of total emissions or emissions per unit of airport area.[1,3] Recently, estimates of average aircraft pollutant concentrations for downwind of airports have been derived,[9,10] based on models in which atmospheric turbulence disperses the exhaust trails of numerous aircraft landing and taking off at the airport. These latter analyses suggest that under some conditions the average concentrations of aircraft pollutants in the downwind direction may be as high as typical present-day levels of these same pollutants in urban atmospheres. Neither of these approaches considers the higher concentrations which may be encountered in the exhaust trail from the time the exhaust leaves the engine until it has been uniformly mixed into the atmosphere with preceding and succeeding trails as envisaged in the farfield dispersion model. This near-field mixing and dispersion process is considered in this paper so that the corresponding estimates of pollutant concentrations could be made if desired.

In subsequent sections we first suggest the model of the combustion process used in further analyses of pollutant production. Subsequently, the formation of nitric oxide is considered and then the formation and oxidation of soot particles. These two pollutants are analyzed in detail because gas turbine combustor operation at full power is better understood than operation at idle. Finally, we treat the dilution of the polluted combustion products with the surrounding atmosphere.

Model of the Combustion Process

The measured exhaust concentrations of nitric oxide and carbon are not related in any simple way to the equilibrium concentrations either within the combustor or at combustor exit. The exhaust concentrations of these two pollutants are determined by rate-limited processes occurring within the combustor, and to follow these processes in detail, a knowledge of the flow pattern and temperature and equivalence ratio distribution within the combustor is required. The main features of this flow are well known, but an adequate quantitative description is not yet available. In this section, the combustion process within the combustor liner is described, and the flow models which we will use for kinetic studies of pollutant production are discussed.

Both can and annular combustors can be divided roughly into two parts, a primary and secondary zone as shown in Fig. 1. In the primary zone, at low altitude and maximum power, about 90% of the fuel is burnt, and the mean fuel/air ratio for this zone is between stoichiometric and slightly fuel-rich. To keep the gas temperature at turbine inlet below about 1300°K, the over-all combustor equivalence ratio is about 0.25. Thus only 20–25% of the total air flow enters the primary zone.

Figure 1 shows the mean flow pattern in a typical combustor. In the primary zone, the largest fraction of the air enters the combustor through swirlers around the fuel spray nozzle. The next largest fraction enters the first row of air holes shown on the top wall of the figure, entrains a fraction of the products of combustion at (2), and drives the recirculating flow pattern which stabilizes the flame. The remainder of the primary zone air is used to film cool the walls of the can. The fuel is sprayed into both the swirler air and the recirculated flow, and at high-pressure combustor operation, combustion is almost complete by (2). Usually the flow at (2) is fuel-rich; and the recirculated flow (3) is somewhat fuel-lean.

In the secondary zone the remaining air is mixed with the primary zone combustion products to complete the combustion of the fuel and to cool the gas stream to the temperature required at turbine inlet. About $\frac{2}{3}$ of the secondary zone air enters the can transverse to the internal flow through large holes in the can wall and mixes in the bulk of the flow. About $\frac{1}{3}$ of the secondary zone air enters parallel to the can, through slots, to film cool the walls as shown in the lower half of Fig. 1.

Detailed models for the primary zone flow have not been sufficiently developed to be of use in chemical kinetic studies, though the basis for an analytical approach can be found, for example, in Refs. 11–13. The simplest approach is to assume a plug flow through the combustor, based on mean primary zone conditions and residence time. This takes no account of variations in temperature, equivalence ratio, and residence times for difference parts of the flow, and can only give a rough estimate of conditions at primary zone exit.

An approach which does make some allowance for a distribution of residence times is to model the primary zone as a well-stirred reactor. Beér and Lee[14] have used the stirred reactor concept to determine the effect of residence time on the performance of a coal-fired furnace. Two limiting cases can be considered: either mixing is complete on a molecular scale, or mixing is only complete on a scale small compared with combustor dimensions, but large compared with molecular dimensions. Thus in the latter case, small fluid elements retain their identity as they pass through the reactor; in the former case complete mixing occurs. The mathematical re-

lations for these reactor models can be found in Beér and Lee's paper.[14]

The secondary zone is considerably easier to model than the primary zone. The calculations in this paper are based on a combustor of the following configuration: a single liner of constant area, circular cross section, with round flush air holes, and surrounded by a constant area circular annulus. It was felt that such an arrangement would serve as a typical combustor. A fluid mechanic and thermodynamic model for this combustor was based on the following assumptions, taken partly from Ref. 15: 1) The flow in the secondary zone is one-dimensional; i.e., all variables are uniform over a cross section. This is an important assumption, as the use of a mean temperature in the chemical kinetic equations will hide the possible freezing of reactions in the cooler zones near the liner wall. 2) All liner air jets mix instantaneously with the combustion products gas stream. In the case of the dilution air, flow visualization studies of combustor mixing (see, e.g. Ref. 12) indicate that this assumption is reasonable. In the case of liner cooling air, however, the jets are purposely directed so as to stay near the liner. But even in this case the liner cooling air is generally replenished every few inches, an indication of the length scale for significant mixing. The distinction between these two types of secondary zone air is shown in Fig. 1. 3) There is no heat transfer from the liner to the annulus. The error made in this assumption will be somewhat corrected by the fact that any heat lost to annulus air is eventually returned to the liner downstream. 4) The only pressure losses in the system are the "hot loss" due to gas expansion and the loss across the liner holes. 5) The density is inversely proportional to the temperature, the effects of molecular weight and pressure variation being ignored. 6) The bulk flow is an equilibrium flow; i.e., its thermodynamic properties and composition of major species are determined by the pressure and mean equivalence ratio at any point along the liner. 7) The liner air hole distribution can be represented as a continuous function of distance along the combustor. The calculations in this paper are based on a uniform distribution of hole area.

With the above assumptions, the fluid mechanic and thermodynamic variables of interest can be calculated as functions of distance from the beginning of the secondary zone. With the axial velocity known throughout the combustor, the flow time for a fluid element (or a particle) starting at the end of the primary zone can be computed. We then have the environmental properties as functions of time, with which we can integrate the kinetic equations for pollutant production (or decomposition). A typical such environmental history is shown in Fig. 5 (along with that for a plug-flow primary zone). The calculations in this paper were based on fuel of the form C_nH_{2n}, burned adiabatically with air initially at 700°K and at a pressure of 15 atm.

Formation of Nitric Oxide

Background

Several investigators and engine manufacturers have measured nitric oxide concentrations in jet engine exhausts (a summary of the data available is given in Ref. 1). The measured exhaust nitric oxide concentrations are about 0.1 times the equilibrium values corresponding to combustion of a stoichiometric mixture of compressor air and fuel which approximates conditions in the primary zone. They may be greater or less than the NO equilibrium concentration at combustor exist, depending on the details of the combustor. These measured concentrations do not correlate satisfactorily with over-all engine equivalence ratio,[8,16] though for a given engine increasing the power level (and hence equivalence ratio) from idle to takeoff does increase the exhaust nitric oxide level.

The nitric oxide formation process in spark-ignition engines is more fully understood, however, and provides a basis for analyzing the gas turbine combustor. Lavoie, Heywood, and Keck[17] have shown how a thermodynamic model for the combustion process in a spark-ignition engine can be combined with a rate equation for nitric oxide formation to give good agreement with measured concentrations of nitric oxide in the engine cylinder. The temperature, pressure, and mean equivalence ratio in the primary zone of a gas turbine combustor are comparable with values attained in the cylinder of the spark-ignition engine so the same kinetic scheme for nitric oxide formation is applicable. However, since the combustion process is fundamentally different, a new thermodynamic model must be derived.

Table 1 Model Reaction Scheme for NO Formation[17]

Reaction[a]	ΔH, kcal/mole	k_i[b], cm³/sec
1) $N + NO \rightleftharpoons N_2 + O$	75.0	2×10^{-11}
2) $N + O_2 \rightleftharpoons NO + O$	31.8	$2 \times 10^{-11} e^{-7.1/RT}$
3) $N + OH \rightleftharpoons NO + H$	39.4	7×10^{-11}
4) $H + N_2O \rightleftharpoons N_2 + OH$	62.4	$5 \times 10^{-11} e^{-10.8/RT}$
5) $O + N_2O \rightleftharpoons N_2 + O_2$	79.2	$6 \times 10^{-11} e^{-24.0/RT}$
6) $O + N_2O \rightleftharpoons 2NO$	36.4	$8 \times 10^{-11} e^{-24.0/RT}$

[a] Exothermic direction left to right.
[b] Exothermic rate constants from Ref. 18 with activation energies in kcal/mole.

Kinetic Model

The set of reactions used by Lavoie et al.,[17] to describe nitric oxide formation in the temperature range 2000–3000°K, pressure range 5–30 atm, and with equivalence ratios close to one in the post-flame gases of a hydrocarbon-air mixture is given in Table 1. The reaction $2NO \rightleftharpoons N_2 + O_2$ is not included since it is slow and does not proceed directly.

To proceed further we need to know the state of the carbon-hydrogen-oxygen system in the burnt gases. The description of the combustion process given suggests that the following assumption is valid. The fluid at the upstream end of the primary zone consists of either unmixed compressor air and the very fuel-rich mixture left behind the evaporating droplets, or of recirculated products and fresh air, again unmixed with the fuel-rich droplet wakes. As the fluid elements move downstream, the air and fuel mix and burn once the equivalence ratio on a molecular scale is within the ignition limits. As we are only considering engine operation at low altitude and maximum thrust, the pressure level is 10–20 atm, and the energy-releasing reactions rapidly go to completion once mixing occurs. We will show shortly that the nitric oxide formation reactions are slow in comparison with the energy-releasing reactions, and we will therefore assume that the burnt gases consist of equilibrium products of combustion corresponding to a local equivalence ratio between stoichiometric (the value at which combustion occurs in a diffusion flame) and the fuel-rich ignition limit of a premixed flame and at the appropriate adiabatic flame temperature.

Rate equations for NO, N, and N_2O can be derived from Table 1 in terms of the species listed. Since we are considering only processes occurring outside the flame-front reaction zone, we will assume the concentrations $[N_2]$, $[O]$, $[O_2]$, $[OH]$, and $[H]$ are given by equilibrium values at the local temperature, pressure, and equivalence ratio. The rate equations then become:

$$(1/V)(d[NO]V/dt) = -\alpha(\beta R_1 + R_2 + R_3 + 2\alpha R_6) + R_1 + \beta(R_2 + R_3) + 2\gamma R_6 \quad (1)$$

$$(1/V)(d[N]V/dt) = -\beta(\alpha R_1 + R_2 + R_3) + R_1 + \alpha(R_2 + R_3) \quad (2)$$

$$(1/V)(d[N_2O]V/dt) = -\gamma(R_4 + R_5 + R_6) + R_4 + R_5 + \alpha^2 R_6 \quad (3)$$

where V is the volume of the small fluid element being fol-

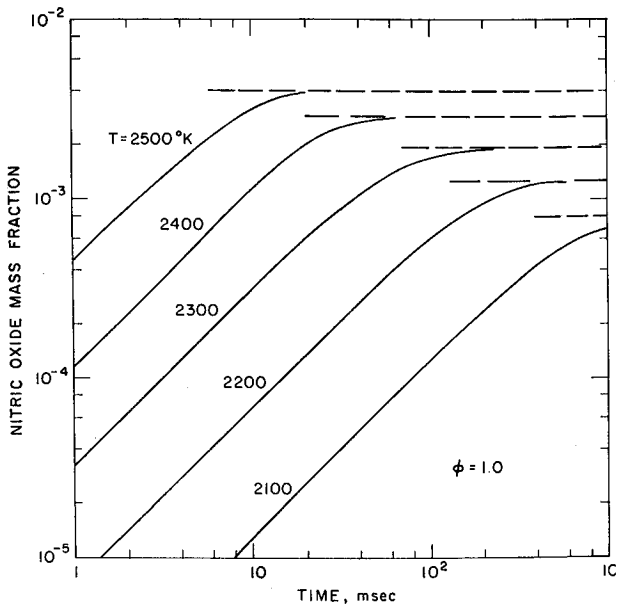

Fig. 2 Calculated NO mass fractions as function of time after combustion for different temperatures and ϕ = 1.0, p = 15 atm; dashed lines are equilibrium NO mass fractions.

lowed through the flow; $\alpha = [NO]/[NO]_e$, $\beta = [N]/[N]_e$, and $\gamma = [N_2O]/[N_2O]_e$ are, respectively, the concentrations of NO, N, and N_2O divided by their equilibrium concentrations; and R_i is the "one-way" equilibrium rate of the ith reaction; e.g., $R_1 = k_1[N]_e[NO]_e$. Rough estimates of the magnitude of the terms in these equations indicate that the relaxation times for the [N] and [N_2O] equations are several orders of magnitude shorter than that for the [NO] equation. It is therefore an excellent approximation to assume steady-state concentrations for N and N_2O and set $d[N]V/dt$ and $d[N_2O]V/dt = 0$. Equations (2) and (3) can then be used to eliminate β and γ from Eq. (1), and the following equation for NO formation results:

$$\frac{1}{V}\frac{d[NO]V}{dt} = 2(1-\alpha^2)\left(\frac{R_1}{1+\alpha K_1} + \frac{R_6}{1+K_2}\right) \quad (4)$$

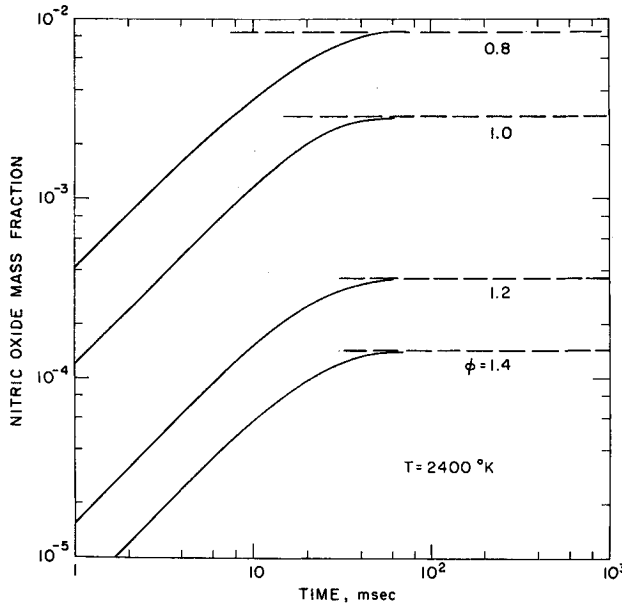

Fig. 3 Calculated NO mass fractions as function of time after combustion for different equivalence ratios and T = 2400°K, p = 15 atm; dashed lines are equilibrium NO mass fractions.

where $K_1 = R_1/(R_2 + R_3)$ and $K_2 = R_6/(R_4 + R_5)$. The first term in the large bracket on the right-hand side of the above equation is the result of reactions 1–3 in Table 1, the extended Zeldovich chain mechanism. The second term is the result of reactions 4–6 and involves N_2O as an intermediary. In general, K_1 and K_2 are of order unity or less, and the relative importance of the two mechanisms just described is determined by the ratio of R_1 to R_6. This is much larger than unity except at low temperatures (less than 2000°K) and lean mixtures. These are the conditions in the dilution zone of the combustor; at these lower temperatures reaction rates are slow, and the nitric oxide concentration is effectively frozen. However, if NO concentrations in the primary zone reach close to equilibrium values, then in the dilution zone α may be greater than unity increasing the relative effect of the R_6 term in Eq. (4).

In the secondary zone, in addition to chemical reaction, the nitric oxide concentration changes as diluting air is mixed with the primary zone combustion products. An extra term must be included in Eq. (4) to allow for this effect. Since the nitric oxide concentration in the diluting air is negligible, the change in concentration due to air addition and mixing can be related to the change in equivalence ratio of each fluid element. Equation (4), rearranged in terms of the mass fraction of nitric oxide, {NO} then becomes

$$\frac{d\{NO\}}{dt} = \frac{2M_{NO}}{\rho}(1-\alpha^2)\left(\frac{R_1}{1+\alpha K_1} + \frac{R_6}{1+K_2}\right) + \frac{\{NO\}}{\phi(1+0.068\phi)}\frac{d\phi}{dt} \quad (5)$$

where the last term gives the change in NO mass fraction due to dilution. M_{NO} is the molecular weight of NO, ρ is the local gas density, and ϕ the local equivalence ratio.

This kinetic model has been programed for solution on a digital computer and linked with a program which calculates equilibrium thermodynamic properties and species concentrations. It can be applied to a steady flow process where the pressure-time, temperature-time, and composition-time histories of the fluid elements in the flow are known.

Numerical Results

Before attempting to model the flow in a gas turbine combustor, it is instructive to consider some results obtained with Eq. (5) for some simpler flows. As a first approximation to our combustion model, we can regard the fluid elements in the flow as combustion products of uniform temperature and composition, but which burn at different times during the flow through the primary zone. Results for nitric oxide mass fraction, as a function of time, for constant temperature and equivalence ratio are shown in Figs. 2 and 3. The pressure is 15 atm. Note that the characteristic formation time is a strong function of temperature (Fig. 2), but a weak function of equivalence ratio (Fig. 3).

Current gas turbine combustor primary zone conditions are approximately equivalence ratio 1.0–1.2, temperature at zone exit 2300–2500°K, and mean residence time of order 5 msec. It is clear that there is insufficient time for nitric oxide concentrations to reach equilibrium. However, any design changes which increase the peak temperatures inside the combustor (e.g., increased engine pressure ratio) will bring NO levels at primary zone exit closer to equilibrium values.

Some conclusions on the effect of air addition at the start of the secondary zone can also be drawn from Eq. (5). As air is mixed with the combustion products, until the equilibrium nitric oxide concentration falls below the rate-limited nitric oxide concentrations, nitric oxide will continue to be formed through the first term in Eq. (5). As the temperature falls, however, the rate of formation decreases rapidly, and at some point the concentration can be regarded as chemically frozen,

and only changes which result from dilution will be important. This freezing point can be estimated as follows.

At the exit of the primary zone for current designs, the nitric oxide concentration is significantly less than the equilibrium concentration. For $\alpha \ll 1$ and $R_6 \ll R_1$, Eq. (5) gives the chemical formation rate as

$$(d\{\mathrm{NO}\}/dt)_{\alpha=0} = 2M_{\mathrm{NO}}R_1/\rho$$

which is a function of pressure, temperature, and equivalence ratio only. Values of $d\{\mathrm{NO}\}/dt$ at $\alpha = 0$ are given in Fig. 4 as a function of temperature for 15 atm pressure and ϕ = 0.6, 0.8, 1.0, and 1.2. The dashed curve shows the adiabatic flame temperature for each equivalence ratio; ideally as air is mixed with the products, the gas temperature would follow this curve. Note that for initially fuel-rich products, the nitric oxide formation rate will increase until $\phi \approx 1.0$, and then will decrease rapidly. The secondary zone residence time is about 5 msec, and a typical maximum NO mass fraction within the combustor is 5×10^{-4}. Thus an NO formation rate of less than about 10^{-2} sec^{-1} will result in a negligible change in NO concentration, and Fig. 4 shows that nitric oxide chemistry is effectively frozen at $\phi \approx 0.7$. The details of the primary zone flow and the early part of the secondary zone determine the exhaust concentration

The preceding paragraphs emphasize the need for a detailed thermodynamic and fluid dynamic model of the primary zone before realistic kinetic calculations for a complete combustor can be carried out. We do not yet have such a model. However, by assuming simple flow patterns for the primary and secondary zones, we have been able to show which parts of the combustor are most important in the nitric oxide formation process.

Simple models for the primary zone—a plug flow or a well-stirred reactor—were described in the previous section. However, for engines with pressure ratios of about 15:1 or less, the nitric oxide concentration in the combustor primary

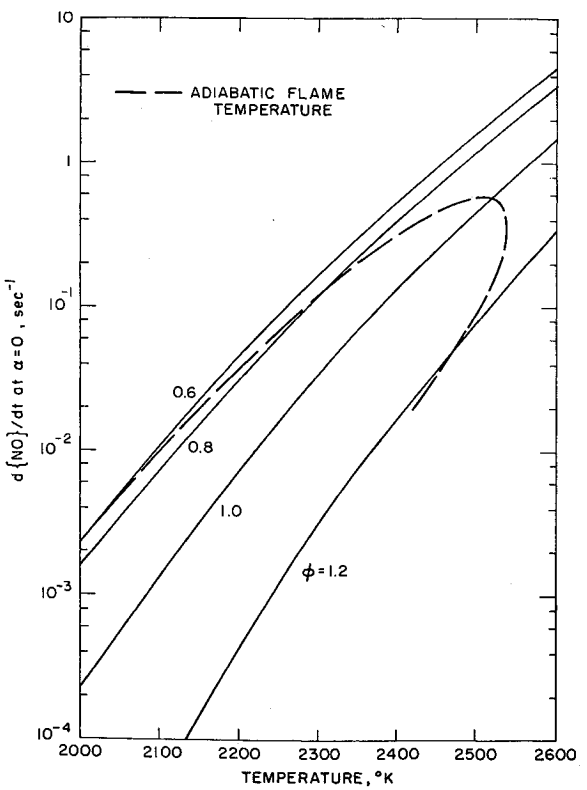

Fig. 4 Rate of change of NO mass fraction (sec^{-1}), for α = 0, as a function of temperature for different equivalence ratios; dashed curve shows adiabatic flame temperature for kerosene-air combustion at 15 atm for 700°K air.

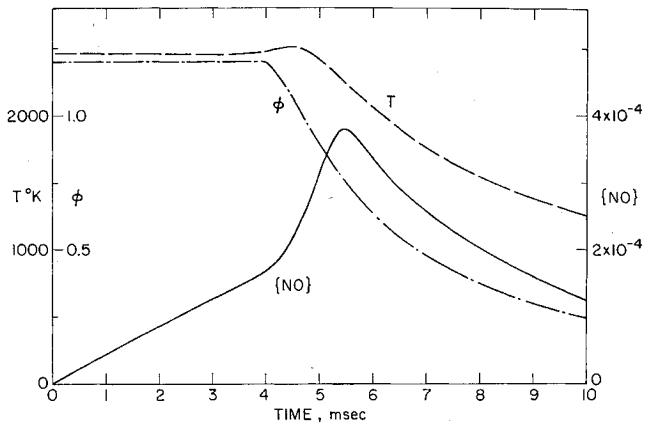

Fig. 5 Temperature, equivalence ratio, and NO mass fraction as function of the time spent by a fluid element in the combustor: 0–4 msec corresponds to the primary zone; 4–10 msec corresponds to secondary zone; pressure equals 15 atm, compressor air at 700°K.

zone is much less than the equilibrium concentration, and Eq. (5) indicates that the formation rate for uniform temperature and equivalence ratio will be almost constant. Under these conditions, the three models described give nitric oxide concentrations at the primary zone exit which differ by less than 10%. Since the assumptions in each model make little difference to the result, the simplest approach—the plug flow—was used. This conclusion would not necessarily hold for combustors with higher peak flame temperatures.

Conditions appropriate for one can of a current large jet engine combustor were chosen, with mean primary zone equivalence ratio equal to 1.2, mean primary zone temperature equal to the adiabatic flame temperature for 700°K, 15 atm compressor air, and primary zone residence time 4 msec. The secondary zone conditions were calculated using the one-dimensional model described earlier with total air mass flow of 17 lb/sec, overall equivalence ratio 0.25, combustor inside diameter 7 in. and combustor length 15 in. The equivalence ratio and temperature distribution inside the combustor and the nitric oxide mass fraction calculated from Eq. (5) are shown in Fig. 5, as functions of the time spent by a fluid element in the combustor.

At the exit of the primary zone, the nitric oxide mass fraction is 29% of the equilibrium concentration at primary zone conditions. In the secondary zone, significantly more nitric oxide is formed as the equivalence ratio changes from 1.2 to about 0.8. At this point the chemistry is effectively frozen, and the concentration only changes due to dilution. The calculated exhaust NO mass fraction is 1.2×10^{-4} and measured values, for example for the JT8D engine to which the calculation approximately corresponds, are about 9×10^{-5} (see Ref. 8).

The nitric oxide behavior which our model predicts in the early part of the secondary zone is different from that described by Sawyer.[16] We have predicted that for a combustor like the JT8D, NO continues to form because the concentration calculated from the NO formation rate equation is less than the local equilibrium concentration. For this combustor, then, it would not be practicable to tailor the initial part of the secondary zone to promote nitric oxide decomposition which was one control technique proposed.

One would expect this simple primary zone model to overestimate the nitric oxide concentration since the actual mean temperature will lie below the theoretical adiabatic flame temperature, and the reaction rate is very temperature sensitive (we estimate that a 100°K temperature decrease gives about a factor of three reduction in nitric oxide concentration). A more detailed model of the primary zone is under investigation, but the agreement between prediction and measurement indicates that the main features of the flow have been correctly described.

Formation and Oxidation of Solid Carbon

Formation

Data relevant to the study of the formation of solid carbon in gas turbine combustors come from three different types of investigations: those examining the details of the chemical kinetics, those studying the carbon output of simple laboratory flames as functions of the operating conditions of the flame, and those recording the carbon output of gas turbine combustors (or engines) as a function of engine-operating parameters and design variables. At this time the state of knowledge of the kinetics of carbon formation is at a very basic level. It is therefore not possible to attempt an analysis of the sort made on nitric oxide formation in the preceding section of this paper. What can be done, however, is to develop a qualitative picture of the important processes in the primary zone which lead to carbon formation. This picture will be based on data from flame studies and will explain the results of combustor exhaust measurements.

MacFarlane et al.[19] give data on the solid carbon output from premixed laboratory flames at pressures up to 20 atm, as a function of equivalence ratio. These data show that little carbon is formed for $\phi < 1.5$ or so, depending on the fuel, and that above this value the amount formed is a strong and increasing function of pressure. Data from confined hydrocarbon diffusion flames also show carbon output increasing with (over-all) equivalence ratio and pressure, though carbon appears at much lower equivalence ratios.[20] Solid carbon does not, however, appear in the equilibrium products of hydrocarbon-air combustion for $\phi < 3$ or so.

In a general sense, therefore, carbon can be regarded as a reaction intermediate whose consumption is very slow relative to the major gas phase reactions. Thus when a hydrocarbon flame is quenched immediately after completion of the important gas phase reactions, as in an unconfined diffusion flame or bunsen-type premixed flame, the carbon oxidation reaction is often never completed. In the gas turbine combustion process the carbon consumption reaction may or may not be frozen before completion depending on how rapidly cooling air is mixed in (as discussed later in this paper). In a general sense, then, the processes controlling the concentrations of solid carbon and NO are similar; whether or not either reaches its equilibrium value is controlled by a kinetic process which is very slow relative to the other important combustion reactions.

At this point a more detailed examination of the processes determining how the fuel mixes and burns with the primary zone air is necessary. The fuel enters the primary zone in the form of droplets with diameters of 50–200 μm and with a speed relative to the hot gases of the order of 70 m/sec. The combustor gases themselves are flowing in a complicated turbulent pattern with velocities of similar magnitude. The gases are at a temperature which is much higher than the boiling point of the fuel, so the droplets begin to vaporize as soon as they enter the combustor. This mass transfer process is greatly enhanced by the relative velocity between the droplets and the gases, which in turn is being reduced by the drag on the droplets. The droplets never come to zero relative velocity, however; their inertia does not allow them to accommodate to the turbulent velocity fluctuations of the gases. Thus, once their injection momentum is gone, they are dragged around by the combustor gases until they have completely evaporated.

During these evaporation and deceleration processes, the droplets cannot burn with a fully enveloping flame (there may be burning in the wake). This can be deduced from the following result of Spalding[21]:

$$U_c/D = 1.4 \times 10^3 \text{ sec}^{-1} \tag{7}$$

where U_c is the critical (maximum) relative velocity which will allow a droplet of diameter D to burn at its stagnation point. The value of the above ratio has been adjusted to a pressure of 15 atm. Although experimentally verified only for droplets with diameters of the order of centimeters, it is applicable for droplets in the size range discussed here. Whether or not the droplets burn, as droplets, will be determined by the relative time scales of the evaporation and deceleration processes. If the droplets have evaporated before their velocity goes below U_c, then no droplet burning can take place. If they slow down before they have evaporated, the turbulent fluctuations of the gases may prevent their burning anyway.

An evaporation time for a droplet is given by the following equation[22]:

$$\tau_e = D_0^2/\lambda \tag{8}$$

where D_0 is the initial droplet diameter, and λ is the so-called evaporation constant and is a function of the thermodynamic and transport properties of the fuel and the surrounding atmosphere, and the droplet's velocity relative to that atmosphere. For the case of a droplet in a hot stagnant atmosphere, the evaporation constant can be calculated from the theory developed by Goldsmith and Penner,[22] among others. The effect of the relative velocity has been studied by several investigators. Eisenklam et al.[23] found

$$\lambda/\lambda_s = [B/(1 + B)](1 + 0.8Re^{1/2})/\ln(1 + B) \tag{9}$$§

where λ_s is the evaporation constant in a stagnant atmosphere, λ includes the effects of motion, Re is the Reynolds number of the droplet, B is the transfer number for the evaporation process, and all properties are evaluated at the mean of the gas and droplet temperatures. While their study covered values of B in the correct range ($B \approx 10$ for a gas turbine droplet), they studied Reynolds numbers which were too low (their studies covered the range $0.1 < Re < 20$ while gas turbine droplets have $Re \approx 240$ when first injected). Ranz and Marshall[24] found the following correlation, for $0 < Re < 200$, but low values of B:

$$\lambda/\lambda_s = 1 + 0.30Sc^{1/3}Re^{1/2} \tag{10}$$

where Sc is the Schmidt number. In our case the above correlations both give $\lambda/\lambda_s \approx 5$ for a droplet when it is first injected. With $D_0 = 150$ μm and $\lambda_s = 0.02$ cm^2/sec, the evaporation time for a typical droplet is roughly 2 msec.

A droplet deceleration time τ_d can be estimated from an equation describing the deceleration:

$$\tau_d = \tfrac{4}{3}(\rho_f/\rho_g)D_0/C_{d_0}U_0 \tag{11}$$

where ρ_f and ρ_g are the fuel and gas densities, C_{d_0} is the initial droplet drag coefficient, and U_0 is the initial droplet velocity. For Reynolds numbers in the range of those for injected fuel droplets, a nonevaporating droplet has the same drag coefficient as a hard sphere at the same Reynolds number (i.e., the effects of internal circulation and shape distortion are negligible),[25] but a correction must be made for the effects of mass transfer. For $Re < 20$ or so, this correction may be estimated using the correction found by Eisenklam et al.[23]:

$$C_d = C_{d_s}/(1 + B) \tag{12}$$

where C_d is the drag coefficient for an evaporating droplet, and C_{d_s} is the drag coefficient for a nonevaporating sphere at the same Reynolds number. In experiments at higher Reynolds numbers, but lower transfer numbers, the drag coefficient has been found to decrease due to evaporation, but not as much as indicated by Eq. (12).[26] Taking the low Reynolds number correlation as a lower bound on the drag coefficient, the value for hard spheres as an upper bound, and using appropriate values for the various other quantities ($\rho_f/\rho_g = 300$, $C_{d_s} = 0.7$), we find 1.2 msec $< \tau_d <$ 13 msec. Since $\tau_e/\tau_d < 2$ or so, it appears that significant evaporation

§ This correlation does not hold as $Re \to 0$.

will take place during the initial deceleration process. Since, for this case, $U_0/U_c \approx 300$, no droplet combustion will take place at that time.

However, the uncertainties in the above calculations indicate that a significant number of droplets might reach nearly stagnant conditions without vaporizing. For this case we must examine whether the turbulent velocity fluctuations will keep them from burning. The characteristic period of these fluctuations can be estimated as $\tau_f \approx D_j/U_j$ where U_j is the air velocity in the air jets near the injector, and D_j is the diameter (or some characteristic lateral dimension) of these jets. Typically $\tau_f \approx 0.5$ msec for a gas turbine primary zone. The magnitude of these fluctuations may be expected to be roughly one-tenth the mean flow speed, which is typical of turbulent shear flows.[27] The time for a droplet to accommodate itself to these fluctuations is the same as the deceleration time, given in Eq. (11), only here the fluctuation velocity is appropriate rather than the injection velocity. In this case the Reynolds number is roughly 20, so Eq. (12) can be used to estimate the drag coefficient. Using the initial diameter as before and appropriate values ($C_{d_s} = 2$, $U_0 = 7$ m/sec), we find $\tau_d \approx 5$ msec. Note that if the diameter at the end of the initial deceleration process is much less than D_0, the droplet has already mostly vaporized, making this calculation unnecessary. Thus, since $\tau_d/\tau_f \approx 10$, a droplet which comes nearly to rest in the turbulent flow, will not be able to keep up with the velocity fluctuations. Here $U_0/U_c \approx 30$, and, therefore, the droplet will not burn until it has almost entirely evaporated.

Based on the above analysis (and recognizing the crudeness of the numbers), we can draw the following picture of combustion in the primary zone. There exists a very fuel-rich region near the injector face (see Fig. 1) where the droplet evaporation is taking place, but where there is little combustion because of a lack of air. Either air (in the case of the swirl air), or air plus hot products [in the case of the mixture in the reverse flow region, (3) in Fig. 1] flows by this fuel-rich zone entraining and mixing with the fuel vapor, and most of the combustion takes place as the flow travels downstream in the outer region of the zone [region (2) in Fig. 1]. However, each bit of fuel must be mixed with about fifteen times its weight of air before it reaches stoichiometric proportions; therefore, considerable burning must take place at high equivalence ratios. The data from laboratory flames indicate that this will result in the formation of solid carbon. Most of the carbon will be formed in the region very close to the fuel spray as there the equivalence ratios will be the highest.

Data on carbon produced in gas turbine combustors tend to confirm this picture. Investigators have shown that the variables most strongly affecting carbon output are operating pressure, mean primary zone equivalence ratio, the distribution of airflow into the primary zone, and the mixing of this air with the fuel vapor. The increase of carbon output with increasing pressure has been demonstrated directly by combustor tests[28-30] and by correlating engine smoke output with compressor pressure ratio for different engines.[30,31] The increase of carbon output with increasing pressure from the burning process on a molecular level, as shown by MacFarlane et al.,[19] undoubtedly accounts for a large part of this effect. Increasing operating pressure on a single combustor also affects the mixing processes, most strongly by causing a collapse of the fuel cone.[32] This collapse confines the fuel vapor to an even narrower region making carbon formation more likely. The effect of spray cone angle has been demonstrated by combustor tests.[28,32,33] Similarly, the effect of increasing the mean primary zone equivalence ratio in increasing smoke formation has been shown by combustor measurements.[30,34] Several recently developed engines have successfully reduced the smoke problem by leaning out the primary zone as a whole, as well as by injecting a significant amount of air directly into the fuel cone to lower the equivalence ratio there and induce more mixing.[30,35]

Carbon Oxidation

The second process determining the amount of smoke in the exhaust of gas turbine engines is the burning of soot particles in hot combustion products. This chemical reaction has been shown to be significant in the combustion products of both fuel-lean and fuel-rich flames.[36-39] That carbon burn-up is important in determining emission levels has already been demonstrated. Toone[28] observed very high carbon concentrations (up to 2600 μg/liter) in the fuel-rich region of the primary zone of an engine exhausting negligible smoke (carbon density in exhaust less than 10 μg/liter). Other investigators have shown substantial decreases in smoke emission with increases of combustor exit temperature,[30,40] apparently due to increased carbon burn-up.

In general, the burning of solid particles is a very complex process. Diffusion of the reactant toward the particle surface, chemisorption of the reactant on the surface, desorption of the products from the surface, and diffusion of the products away from the surface may all be important. Furthermore, if the number density of particles is high enough, coagulation of smaller particles to form larger ones may occur. Which of these phenomena will be significant depends on the temperature, pressure, and composition of the environment of the particle, the particle size, and the number density of the particles.

Particle sizes in gas turbine exhausts have been examined by several investigators. DeCorso et al.[32] found typical particle diameters of 0.05–0.06 μm, with occasional particles up to 0.125 μm and that these small particles could agglomerate to irregularly shaped clusters with dimensions of 0.6–0.8 μm. Durrant[7,31] discusses spherical particles with diameters of 0.01–0.08 μm. Faitani[30] found particles of 0.1 μm diameter. Lieberman[41] measured particle diameters in the exhaust of a regenerative turbine system and found particles of regular and irregular shape, with diameters up to 1 μm. The composition of these exhaust particles has been measured by several of the above investigators, and others, and it is generally agreed that they consist of about 96% carbon by weight.[30]

There exists a large amount of published data on the burn-up of carbon particles of macroscopic size (up to 1 in.) in hot gas streams (see Ref. 42 for a summary), but the data available on particles of the size found in turbine exhaust are limited. One fact that is known with some certainty is that diffusion plays little part in controlling the rate of soot combustion. In Ref. 42 it is shown that diffusion is unimportant in the combustion of carbon particles with diameters less than about 25 μm. Similarly, it has been observed in experiments that coagulation is not important in the regions of a carbon-producing flame where oxidation is significant (it is known, however, that coagulation is important where carbon is being produced).[36] Thus investigators of soot combustion have had to concern themselves only with determining surface reaction rates.

Three major investigations of soot particle burning rates have come to the authors' attention: the work of Lee, Thring, and Beér,[36] Fenimore and Jones,[37] and Tesner and Tsibulevsky.[38,39] Each group has examined soot oxidation in product gases of various stoichiometries, pressures, and temperatures. The region of oxygen partial pressure and temperature studied by each group is shown in Fig. 6, along with the region of interest in gas turbine combustors (the region shown by Tesner and Tsibulevsky was estimated as they did not report p_{O_2} in their publications). It can be seen that all the investigations have been at oxygen partial pressures and temperatures which are lower than gas turbine conditions. Lee, Thring, and Beér were able to correlate their data for specific reaction rate as linear in oxygen partial pressure, in the form

$$\omega = 1.085 \times 10^4 (p_{O_2}/T^{1/2}) \exp(-39300/RT) \quad (13)$$

where ω is the specific reaction rate (g cm^{-2} sec^{-1}), p_{O_2} is the

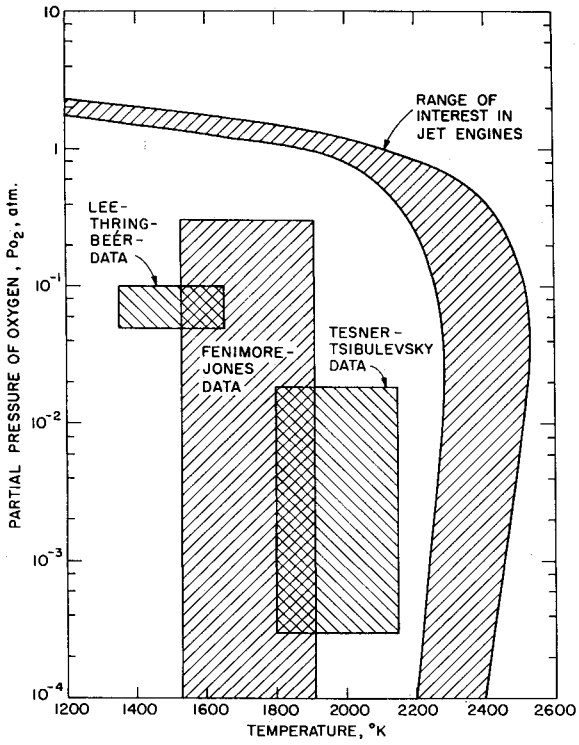

Fig. 6 Regions of available carbon oxidation data compared with region of interest in jet engines.

partial pressure of oxygen (atm), and T is the temperature (°K). They found this correlation to hold over their entire range of investigation. Fenimore and Jones covered a wider range of p_{O_2} and found that, even at conditions investigated by Lee, Thring, and Beér, p_{O_2} was not an important variable. They were able to correlate their data with the assumption that the OH radical is the important reactant, and that some fraction α of the collisions of OH radicals with the particle surface resulted in the removal of a carbon atom. This leads to an expression for specific reaction rate of the form

$$\omega = 1.27 \times 10^2 \alpha p_{OH}/T^{1/2} \quad (14)$$

where p_{OH} is the partial pressure of the OH radical (same units as before). α was found to be 0.1. Tesner and Tsibulevsky could not correlate their data over the whole range of their experiments, but found the specific reaction rate to be linearly dependent on the partial pressure of CO_2 in the lower temperatures of their studies (1800–1940°K). In spite of the fact that available data were not taken in the range of interest, it was felt that the use of the above two burning-rate expressions [Eqs. (13) and (14)] at gas turbine combustor conditions would give at least an estimate of the ability of a gas turbine combustor to consume the carbon it had created.

Figure 7 shows the burning rate expressions evaluated for particles in the products of C_nH_{2n}-air combustion for typical gas turbine conditions (air initially at 700°K and 15 atm pressure) as a function of the equivalence ratio of the product gas mixture. The data are expressed as surface recession rates,

$$dr/dt = -10^4 \omega/\rho_s \quad (15)$$

where dr/dt is the surface recession rate in μm/sec and ρ_s is the density of the soot in g/cm³ (2.25 g/cm³ was used). For a spherical particle dr/dt is the rate of change of the radius. Though there are significant differences between the two correlations, in the most important region $0.7 < \phi < 1.1$, the predictions are of comparable magnitude. It was not expected that the Lee-Thring-Beér correlation would hold for rich mixtures since all their data were taken in the presence of significant O_2 concentrations.

These burning rates indicate what was previously observed experimentally, that a significant amount of the soot produced in the fuel-rich regions of the primary zone can be consumed in the other regions of the primary zone and in the secondary zone. For example, a spherical particle spending 3 msec in near-stoichiometric ($0.8 < \phi < 1.2$) products in the primary zone would undergo a radius change of about 0.1 μm (using the Fenimore-Jones data). The burning rate expressions were integrated numerically for particles travelling through the secondary zone using the fluid mechanic model previously discussed. For mean primary zone equivalence ratios of 0.9–1.2, the Lee-Thring-Beér data gave a radius change of 0.2 μm in the secondary zone; the Fenimore-Jones data gave a radius change of from 0.05 μm for the lean primary zone to 0.08 for the rich. Nonspherical particles could undergo larger size reductions. A comparison of the calculated radius changes with particle sizes observed indicates that carbon oxidation plays an important role in determining the smoke emission level of a combustor. If the data from these extrapolated correlations are correct, then, to reach the exhaust without being consumed, a soot particle may have to spend most of its time travelling in the relatively cooler areas of the combustor near the liner.

Nearfield Dispersion of Jet Engine Trails

The relationship between the rate at which pollutants are emitted by a jet aircraft and the concentration of these pollutants near an airport is determined by the mixing of the jet exhaust with the surrounding atmosphere. There are several physical effects simultaneously acting to determine the ground level concentration: 1) the entrainment of surrounding air and its mixing with the exhaust gases caused by the turbulent motion of the jet trail; 2) the gradual rise of the jet trail due to its buoyancy; 3) the additional mixing of the trail and surrounding air caused by turbulence present in the atmosphere; and 4) the convection of the trail due to the wind. Here we are concerned only with the early stages of mixing in which the first two effects are dominant. There are certain similarities between the flow in a cross wind of the hot exhaust gases from a smoke stack (a stationary source in a moving fluid) and the motion of a trail laid down by a jet aircraft (a moving source in a relative by stationary atmosphere). Adopting an approach similar to that used for tall stack plumes,[43,44] we first propose to analyze theoretically the turbulent mixing of a jet trail in a stationary, nonturbulent atmosphere with no stratification (neutrally buoyant).

The basic theory for this motion is a simple extension of that used successfully to correlate field data for plumes from tall stacks.[44] Consider a single jet engine moving horizontally at a constant speed V, which initially lays down a trail having a horizontal momentum per unit length of m_i and thermal

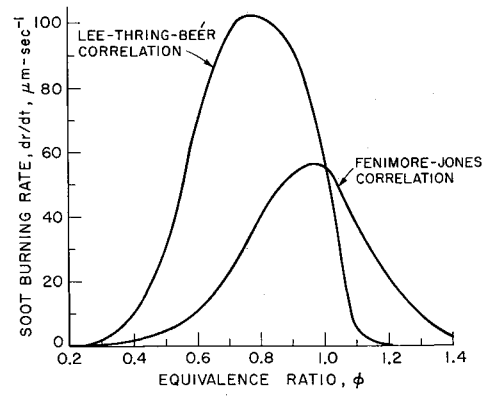

Fig. 7 Calculated burning rates of soot particles, in adiabatic combustion products of kerosene (C_nH_{2n}) and 700°K air at 15 atm.

energy per unit length of e_i. We are concerned with the growth and rise with time of a section of the trail at a fixed axial location with respect to the ground. Considering the fluid in the trail to have a mean horizontal velocity v and vertical velocity u inside a cylindrical region of radius b, the growth by entrainment is hypothesized to be

$$(d/dt)(\pi b^2) = 2\pi b(\beta u + \alpha v) \tag{16}$$

in which α and β are constants of order one, to be determined from experiments. (A discussion of such entrainment hypotheses is given in Ref. 44.) We have assumed v and $u \ll V$, and $\rho_0 - \rho \ll \rho_0$, ρ_0 being the ambient atmospheric density. The conservation of energy requires that

$$(d/dt)(\pi b^2[T - T_0]) = 0 \tag{17}$$

in which $T - T_0$ is the temperature excess above the value T_0 of the surrounding atmosphere. With $T - T_0 \ll T_0$, linearized versions of the horizontal and vertical momentum equations are

$$(d/dt)(\pi b^2 v) = 0 \tag{18}$$

$$(d/dt)(\pi b^2 u) = \pi b^2 g(T - T_0)/T_0 \tag{19}$$

where g is the acceleration due to gravity.

The equations of conservation of energy [Eq. (17)] and horizontal momentum [Eq. (18)] may be integrated to give

$$\pi b^2(T - T_0) = e_i/\rho_0 c_p \tag{20}$$

$$\pi b^2 v = m_i/\rho_0 \tag{21}$$

in which c_p is the constant pressure specific heat. As a consequence the vertical momentum Eq. (19) integrates to

$$\pi b^2 u = g e_i t/\rho_0 c_p T_0 \tag{22}$$

if it is assumed that there is no initial vertical momentum. By introducing a characteristic time τ and length scale l defined by

$$\tau \equiv m_i c_p T_0/g e_i \tag{23}$$

and

$$l^3 \equiv m_i^2 c_p T_0/\rho_0 g e_i = m_i \tau/\rho_0 \tag{24}$$

the trail radius b and the vertical rise z can be obtained by integration of the entrainment Eq. (16), assuming both are zero at $t = 0$, to give

$$(b/l)^3 = (3/\pi)[(\beta/2)(t/\tau)^2 + \alpha(t/\tau)] \tag{25}$$

$$\frac{z}{l} = \frac{1}{l}\int_0^t u\,dt = \left(\frac{\pi}{9}\right)^{1/3} \int_0^{t/\tau} \frac{x\,dx}{\{(\beta/2)x^2 + \alpha x\}^{2/3}} \tag{26}$$

For times small compared with τ, b, and z are less than l and vary as $t^{1/3}$ and $t^{4/3}$, respectively, while for times long compared with τ both b and z are larger than l and vary as $t^{2/3}$. Physically, for times small compared with τ, the trail entrainment is due mostly to the horizontal velocity v while for longer times it is due mostly to the vertical speed u. Thus initially the trail behavior is determined by the jet momentum, but eventually the effects of buoyancy predominate. A numerical calculation for b and z is shown in Fig. 8.

The time τ and the scale l may now be related to the jet thrust F, the flight speed V, and the fuel heat rate q through the initial momentum and energy deposition per unit length,

$$m_i = F/V \tag{27}$$

$$e_i = q/V \tag{28}$$

giving

$$\tau = F c_p T_0/qg \tag{29}$$

$$l = (F\tau/\rho_0 V)^{1/3} \tag{30}$$

The fuel rate per unit thrust is nearly the same for most jet engines, having a value of about 0.8 lb fuel/hr per lb thrust. Thus the time τ is essentially the same for all engines at all flight speeds, having a value of about 30 sec. The corresponding length scale l varies with thrust and speed, but has a value of about 30 m when F = 15,000 lb and V = 120 knots.

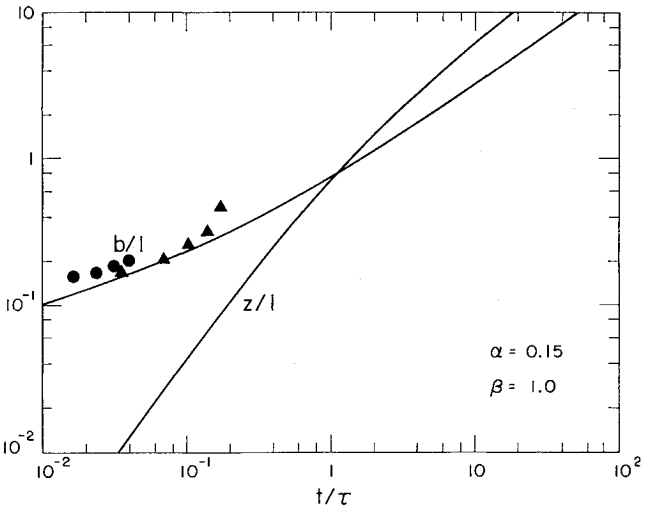

Fig. 8 Jet trail radius b, and rise z as a function of time t: characteristic time τ and length scale l are defined by Eqs. (29) and (30).

Based on this elementary theory of jet trail growth due to its own turbulent motion, at takeoff the trail grows quickly to a radius of about 100 ft in a half minute, then more slowly, requiring about ten minutes to grow to a radius of 1000 ft.

Some preliminary measurements of jet trail growth were made from photographs of smokey exhaust trails of commercial 727 aircraft after takeoff. The measured trail radius is compared in Fig. 8 with the theoretical calculations based on Eqs. (25, 29, and 30). F is assumed to be the total thrust of all engines, and τ and l were estimated to be 56 sec and 153 ft, respectively.

This simple theory does not take into account the effects of high-speed jet mixing near the jet engine, the interaction of multiple engines, nor the motions induced by the wing.

Conclusions

This paper has discussed in detail the basic physical processes which determine emission levels of solid carbon and nitric oxide from gas turbine engines and has given a simple theory for the dispersion of pollutants from the jet trail. The quantitative results should, however, be regarded as preliminary since several areas require further study. These areas are: the fluid mechanics and thermodynamics of the primary zone, the chemical kinetics of pollutant formation and consumption, and the interaction of the jet trail with a turbulent stratified atmosphere. Since the emission of pollutants by aircraft is a cause for public concern, further work in these areas is both necessary and timely.

References

[1] Bastress, E. K. and Fletcher, R. S., "Nature and Control of Aircraft Engine Exhaust Emissions," Rept. 1134-1, 1968, Northern Research and Engineering Corp., Cambridge, Mass.

[2] Nolan, M., "A Survey of Air Pollution in Communities Around the John F. Kennedy International Airport," June 1966, Robert H. Taft Sanitary Engineering Center, Public Health Service, Cincinnati, Ohio.

[3] Cohan, W. J., "Nature and Control of Aircraft Engine Exhaust Emissions," Senate Document 91-9, 1969, U. S. Govt. Printing Office, Washington, D. C.

[4] George, R. E., Verssen, J. A., and Chass, R. L., "Jet Air-

craft: A Growing Source of Pollution," *Journal of Air Pollution Control Association*, Vol. 19, No. 11, 1969, pp. 847–855.

[5] Lozano, E. R., Melvin, W. W., and Hochheiser, S., "Air Pollution Emissions from Jet Engines," *Journal of Air Pollution Control Association*, Vol. 18, 1968, pp. 392–394.

[6] George, R. E. and Burlin, R. M., "Air Pollution from Commercial Jet Aircraft in Los Angeles County," April 1960, Los Angles Air Pollution Control District, Los Angeles, Calif.

[7] Durrant, T., "The Control of Atmospheric Pollution from Gas Turbine Engines," Preprint 680347, April 1968 Society of Automotive Engineers.

[8] Smith, D., Sawyer, R. F., and Starkman, E. S., "Oxides of Nitrogen from Gas Turbines," *Journal of Air Pollution Control Association*, Vol. 18, 1968, pp. 30–35.

[9] Fay, J. A., "Air Pollution from Future Giant Jetports," Air Pollution Control Association Paper 70-78, June 1970.

[10] Milford, N. et al., "Air Pollution by Airports," Grumman Research Dept. Rept. RE-383J, 1970, Grumman Aerospace Corp., Bethpage, N. Y.

[11] Clarke, J. S., "The Relation of Specific Heat Release to Pressure Drop in Aero-gas-turbine Combustion Chambers," *Joint Conference on Combustion*, Institute of Mechanical Engineering and ASME, 1955, pp. 354–361.

[12] Winter, E. F., "Flow Visualization Techniques Applied to Combustion Problems," *Journal of Royal Aeronautical Society*, Vol. 62, 1958, pp. 270–276.

[13] Kind, C. and Youssef, T., "Calculating the Flow in the Combustion Chambers of Gas Turbines," *Brown Boveri Review*, Vol. 51, 1964, pp. 808–816.

[14] Beér, J. M. and Lee, K. B., "The Effect of the Residence Time Distribution on the Performance and Efficiency of Combustors," *10th Symposium (International) on Combustion*, The Combustion Institute, 1965, pp. 1187–1202.

[15] Graves, C. C. and Grobman, J. S., "Mathematical Analysis of Total-Pressure Loss and Airflow Distribution for Tubular Turbojet Combustors with Constant Annulus and Liner Cross-Sectional Areas," Rept. 1373, 1958, NACA.

[16] Sawyer, R. F., "Fundamental Processes Controlling the Air Pollution Emissions from Turbojet Engines," AIAA Paper 69-1040, Anaheim, Calif., 1969.

[17] Lavoie, G. A., Heywood, J. B., and Keck, J. C., "Experimental and Theoretical Study of Nitric Oxide Formation in Internal Combustion Engines," *Combustion Science and Technology*, Vol. 1, 1970, pp. 313–326.

[18] Schofield, K., "An Evaluation of Kinetic Rate Data for Reactions of Neutrals of Atmospheric Interest," *Planetary and Space Science*, Vol. 15, 1967, pp. 643–670.

[19] MacFarlane, J. J., Holderness, F. H., and Whitcher, F. S. E., "Soot Formation Rates in Premixed C_5 and C_6 Hydrocarbon Air Flames at Pressures up to 20 Atmospheres," *Combustion and Flame*, Vol. 8, 1964, pp. 215–229.

[20] Schalla, R. L. and Hibbard, R. R., "Smoke and Coke Formation in the Combustion of Hydrocarbon-Air Mixtures," Chap. IX, Rept. 1300, 1957, NACA.

[21] Spalding, D. B., "Experiments on the Burning and Extinction of Liquid Fuel Spheres," *Fuel*, Vol. 32, 1953, pp. 169–185.

[22] Goldsmith, M. and Penner, S. S., "On the Burning of Single Drops of Fuel in an Oxidizing Atmosphere," *Jet Propulsion*, Vol. 24, 1954, pp. 245–251.

[23] Eisenklam, P., Arunachalam, S. A., and Weston, J. A., "Evaporation Rates and Drag Resistance of Burning Drops," *Eleventh Symposium (International) on Combustion*, The Combustion Institute, Pittsburgh, Pa., 1967, pp. 715–728.

[24] Ranz, W. E. and Marshall, W. R., "Evaporation from Drops," *Chemical Engineering Progress*, Vol. 48, 1952, pp. 141–146, 173–180.

[25] Graves, C. C. and Scull, W. E., *Design and Performance of Gas Turbine Power Plants*, edited by W. R. Hawthorne and W. T. Olson, Princeton University Press, Princeton, N. J., 1960, pp. 166–244.

[26] Ingebo, R. D., "Atomization, Acceleration, and Vaporization of Liquid Fuels," *Sixth Symposium (International) on Combustion*, The Combustion Institute, 1957, pp. 684–687.

[27] Townsend, A. A., *The Structure of Turbulent Shear Flow*, Cambridge University Press, London, 1956.

[28] Toone, B., "A Review of Aero Engine Smoke Emission," *Cranfield International Symposium Series*, Vol. 10; *Combustion in Advanced Gas Turbine Systems*, edited by I. E. Smith, Pergamon Press, New York, 1968.

[29] Butze, H. F., "Effect of Inlet-Air and Fuel Parameters on Smoking Characteristics of a Single Tubular Turbojet Engine Combustor," RM E52A18, 1952, NACA.

[30] Faitani, J. J., "Smoke Reduction in Jet Engines through Burner Design," Paper 680348, 1968, Society of Automotive Engineers.

[31] Durrant, T., "The Reduction of Smoke from Gas Turbine Engines," presented to 9th International Aeronautical Congress, A.F.I.T.A.E., Paris, June 1969.

[32] DeCorso, S. M., Hussey, C. E., and Ambrose, M. J., "Smokeless Combustion in Oil Burning Gas Turbines," Paper 67-PWR-5, 1957, ASME.

[33] Lefebvre, A. H. and Durrant, T., "Design Characteristics Affecting Gas Turbine Combustion Performance," presented to National Aeronautical Meeting, SAE, Los Angeles, Oct. 1960.

[34] Gleason, J. G. and Faitani, J. J., "Smoke Abatement in Gas Turbine Engines through Combustor Design," Paper 670200, 1967, Society of Automotive Engineers.

[35] Bahr, D. W., Smith, J. R., and Kenworthy, M. J., "Development of Low Smoke Emission Characteristics for Large Aircraft Turbine Engines," AIAA Paper 69-493, U. S. Air Force Academy, Colo., 1969.

[36] Lee, K., Thring, M., and Beér, J., "On the Rate of Combustion of Soot in a Laminar Soot Flame," *Combustion and Flame*, Vol. 6, 1962, pp. 137–145.

[37] Fenimore, C. P. and Jones, G. W., "Oxidation of Soot by Hydroxyl Radicals," *Journal of Physical Chemistry*, Vol. 71, 1967, pp. 593–597.

[38] Tesner, P. A. and Tsibulevsky, A. M., "Kinetics of Dispersed Carbon Gasification in Diffusion Flames of Hydrocarbons," *Combustion and Flame*, Vol. 11, 1967, pp. 227–233.

[39] Tsibulevsky, A. M. and Tesner, P. A., "Gasification of Dispersed Carbon in Hydrocarbon Diffusion Flames," *Combustion, Explosion and Shock Waves*, Vol. 2, 1966, pp. 38–42.

[40] Gross-Gronowski, L., "Smoke in Gas-Turbine Exhaust," Paper 67-WA/GT-5, 1967, ASME.

[41] Lieberman, A., "Composition of Exhaust from a Regenerative Turbine System," *Journal of Air Pollution Control Association*, Vol. 18, 1968, pp. 149–153.

[42] Essenhigh, R. H., Froberg, R., and Howard, J. B., "Combustion Behavior of Small Carbon Particles," *Industrial and Engineering Chemistry*, Vol. 57, 1965, pp. 32–43.

[43] Hoult, D. P., Fay, J. A., and Forney, L. J., "A Theory of Plume Rise Compared with Field Observations," *Journal of Air Pollution Control Association*, Vol. 19, No. 8, 1969, pp. 585–590.

[44] Fay, J. A., Escudier, M., and Hoult, D. P., "A Correlation of Field Observations of Plume Rise," *Journal of Air Pollution Control Association*, Vol. 20, No. 6, 1969, pp. 391–397.